Science of the Total Environment 789 (2021) 147935

Contents lists available at ScienceDirect

Science of the Total Environment

journal homepage: www.elsevier.com/locate/scitotenv

Assessment of the effects of straw burning bans in China: Emissions, air quality, and health impacts

Ling Huang [a,b], Yonghui Zhu [a,b], Qian Wang [a,b], Ansheng Zhu [a,b], Ziyi Liu [a,b], Yangjun Wang [a,b], David T. Allen [c], Li Li [a,b,*]

[a] School of Environmental and Chemical Engineering, Shanghai University, Shanghai 200444, China
[b] Key Laboratory of Organic Compound Pollution Control Engineering (MOE), Shanghai University, Shanghai 200444, China
[c] Center for Energy and Environmental Resources, University of Texas at Austin, 10100 Burnet Road, Austin, TX 78758, United States

HIGHLIGHTS

- The effects of straw burning bans on air quality and health benefit in China is assessed.
- Total $PM_{2.5}$ emissions from OCSB decreased by 47% due to straw burning bans, although substantial regional differences exist.
- Avoided number of premature deaths due to straw burning bans was estimated to be 4,256 on a national scale.

GRAPHICAL ABSTRACT

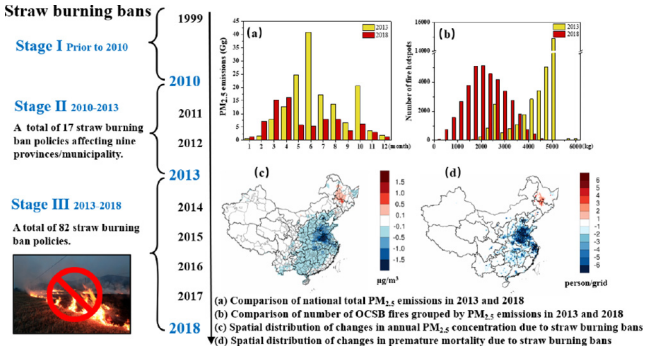

ARTICLE INFO

Article history:
Received 12 March 2021
Received in revised form 13 May 2021
Accepted 18 May 2021
Available online 21 May 2021

Editor: Pavlos Kassomenos

Keywords:
Open biomass burning
Emissions
Air quality
Health benefit
China

ABSTRACT

Open biomass burning (OBB) plays an important role in air pollution and climate change by releasing short-term but intensive amounts of particulate matter and gaseous air pollutants. During past years, policies with respect to prohibition on open straw burning have been issued in China in order to mitigate the air pollution problems and the effectiveness of these straw burning bans in different regions remains to be evaluated. In this study, open crop straw burning (OCSB) emissions during 2010–2018 were analyzed based on a commonly used emission inventory with high spatial and temporal resolution. High emissions concentrated over Northeast China (31.8% of national total $PM_{2.5}$ emissions in 2018), East China (24.0%), and North China (16.6%). Simulations based on an integrated meteorology-air quality modeling system and an exposure-response function show that OCSB emissions could increase monthly $PM_{2.5}$ concentration by as much as 10 μg/m^3 during burning seasons in Northeast China and were associated with 4741 premature deaths in 2018. Spatial heterogeneities were observed with respect to the trends of OCSB emissions during 2010–2018. In East China, North China, and Central China, OCSB emissions showed a general declining trend since 2013 while an opposing increasing trend was observed in Northeast China with peak emissions in 2017. Comparing 2013 (before intensive implementation of straw burning bans) and 2018 (after), national total $PM_{2.5}$ emissions from OCSB activities decreased by 46.9%, ranging from −14.1% to +70% depending on the specific regions. Northeast China is the only region that showed higher OCSB emissions in 2018 compared to 2013, probably associated with the relatively delayed implementation of the straw burning bans. Avoided number of premature deaths due to reduced OCSB emissions was estimated to be 4256 on a national scale, with

* Corresponding author at: School of Environmental and Chemical Engineering, Shanghai University, Shanghai 200444, China.
E-mail address: lily@shu.edu.cn (L. Li).

https://doi.org/10.1016/j.scitotenv.2021.147935

most health benefits gained in East and Central China. Results from this study demonstrate the importance of OCSB contribution to $PM_{2.5}$ concentrations and spatial heterogeneities exist in terms of the effectiveness of the straw burning bans in reducing OCSB emissions and gained health benefits.

1. Introduction

Open biomass burning (OBB), including forest fires, grassland fires, shrub fires, and crop straw burning, represent an important source of fine particulate matter ($PM_{2.5}$, aerodynamic diameters less than 2.5 μm) and trace gases that could have substantial impacts on atmospheric chemistry, regional climate and public health (Zha et al., 2013; Zong et al., 2016; Zhou et al., 2017). Bond et al. (2004) found that the emissions from OBB accounted for 26–73% of global total PM and 33–41% of fine black carbon (BC) while Wiedinmyer et al. (2011) calculated contribution of OBB to global BC, carbon monoxide (CO), and organic carbon (OC) emissions by 72%, 33%, and 62% in 2008, respectively. Streets et al. (2003) estimated that the amount of biomass burned in Asia in 2000 was 730 Tg and 250 Tg was due to open burning of crop residues, of which China and India accounted for 110 Tg and 84 Tg of burning residues, respectively.

As a major method to remove crop residues, provide fertilization, and manage pests (Korontzi et al., 2006), open crop straw burning (OCSB) constitutes an important part of OBB activities and is very common in peri-urban and rural areas (Yevich and Logan, 2003; Yin et al., 2021). During 2001 and 2003, the Russian Federation accounts for 31–36% of global agriculture fires, making it the largest contributor to agriculture burning (Korontzi et al., 2006). In southeastern Asian countries, such as India, Thailand, Philippine, agricultural burning activities are also very active (Gadde et al., 2009; Kumar et al., 2015). Being a large agricultural country, China also has huge biomass burning emissions, especially associated with OCSB. It is reported that nearly 100 million tons of biomass in China is burned in the open fields every year (Zhang et al., 2015) and OCSB in China accounts for approximate 20% of global agricultural waste burning emissions (Hong et al., 2016). From 2002 to 2016, the annual emissions of various air pollutants (e.g. BC, OC, $PM_{2.5}$, etc.) from OCSB have been continuously increasing by ~200% in China (Mehmood et al., 2018). Meanwhile, rapid industrialization and urbanization over the past several decades have led to frequent occurrences of severe haze pollution with high $PM_{2.5}$ concentrations in China (Li and Zhang, 2014; Wu et al., 2016; Bei et al., 2020; Gao et al., 2020; Shen et al., 2020). Many studies have shown that OBB plays an important role during heavy haze episodes, especially during the post-harvest season when agriculture burning activities are intense (Cheng et al., 2014; Zhou et al., 2018; Yang et al., 2020). For example, Cheng et al. (2014) found that from 28 May to 6 June 2011, OBB contributed 37% of $PM_{2.5}$ observed concentrations in the Yangtze River Delta (YRD) region. Zhou et al. (2018) investigated the intense biomass burning events in the North China Plain and found that OCSB contributed an average of 19% to $PM_{2.5}$ concentration in Beijing during a severe haze episode of October 2014. Yang et al. (2020) showed that in Northeast China the contribution of OBB to $PM_{2.5}$ concentration was 52.7% during the post-harvest season in November 2015.

Although still under debate, open straw burning has been banned in many regions or countries, such as the U.S., European Union, China, India, Austria, and Southeast Asia (Pollution Control Department, 2012; Vagg, 2015; Pandey et al., 2017; Tore, 2019), with the aim of reducing CO_2 emissions and mitigating smog problems. Junpen et al. (2018) assessed the trends of paddy field areas burned in Thailand during 2010–2017 and a decreasing trend was observed since 2012 as the result of bans imposed on crop residue burning and promotion of utilization of crop residue. Seglah et al. (2020) indicates that the current crop straw utilization is not effectively practiced in Northern region of Ghana and consistent policies with respect to prohibition of field straw burning are needed across all regions of Ghana. In 2013, the State Council of China issued the "Air Pollution Prevention Action Plan", which requires "to realize comprehensive utilization of rural waste and to reduce open burning of crop straw". In 2013 and 2015, the National Development and Reform Commission of China successively issued the "Notice on Strengthening the Comprehensive Utilization of Crop Straw and Banning of Crop Burning" and the "Notice on Further Accelerating the Comprehensive Utilization of Crop Straw and Banning of Crop Burning" with strengthened supervision and financial support to control OCSB activities. Since then, more and more straw burning relevant policies have been issued by provincial or municipal government across China (e.g. "Notice on the Promotion and Release of Ten Models for Straw Farming" in China, "Action Plan for Straw Treatment in Northeast China" in provinces of Liaoning, Heilongjiang and Jilin). Thus, it is of great importance to evaluate the effectiveness of these control policies in order to help the policy makers to adjust current policies and formulate future ones. However, while spatial heterogeneities of the implementation of straw burning bans exist across different parts of China, very limited studies have assessed the impacts of straw burning bans on OCSB activities and subsequent air quality at the national scale (Sun et al., 2019; Yang et al., 2020).

In this study, we first presented the spatial and temporal trends of OCSB emissions in China for the period of 2010–2018 based on a frequently used emission inventory. An integrated meteorological and air quality model was applied to (1) quantify the contribution of OCSB emissions to $PM_{2.5}$ concentrations and (2) evaluate the impacts of straw burning bans on $PM_{2.5}$ concentrations. An exposure-response function was further applied to estimate the health impacts associated with OCSB and the implementation of straw burning bans. Results from this study provide valuable information for formulating effective strategies to mitigate air pollution and associated health impacts in China as well as other regions of the world where OCSB emissions are also intense (e.g. India, Iran, Saudi Arabia).

2. Methodology

2.1. Straw burning bans in China

The development of China's control policy related to prohibition on open straw burning and straw utilization (together referred as straw burning bans) can be roughly divided into three stages (Fig. 1). In 1999, China's Environmental Protection Administration and five other departments jointly formulated the "Measures for the Management of Prohibition of Burning and Comprehensive Utilization of Crop Straw", as the first national policy to emphasize open straw burning. Prior to 2010 (Stage I), only a few straw burning policies were formulated. During Stage II (2010—2013), the "Twelfth Five-Year Plan for Comprehensive Utilization of Crop Straw Implementation Plan" was released in 2011, with emphasis on the expansion of areas with prohibited straw burning and increased capital investment for straw utilization. A total of 17 relevant policies were formulated at national or provincial level (nine provinces/municipality affected: Henan, Hunan, Jiangsu, Shanghai, Hebei, Tianjin, Jilin, Gansu, Qinghai) during this stage and nearly half of the policies were issued in East China, including Jiangsu and Shanghai. With the release of the "Air Pollution Prevention Action Plan" by the State Council in 2013, the number of policies related to straw burning prohibition grew exponentially. During 2013–2018

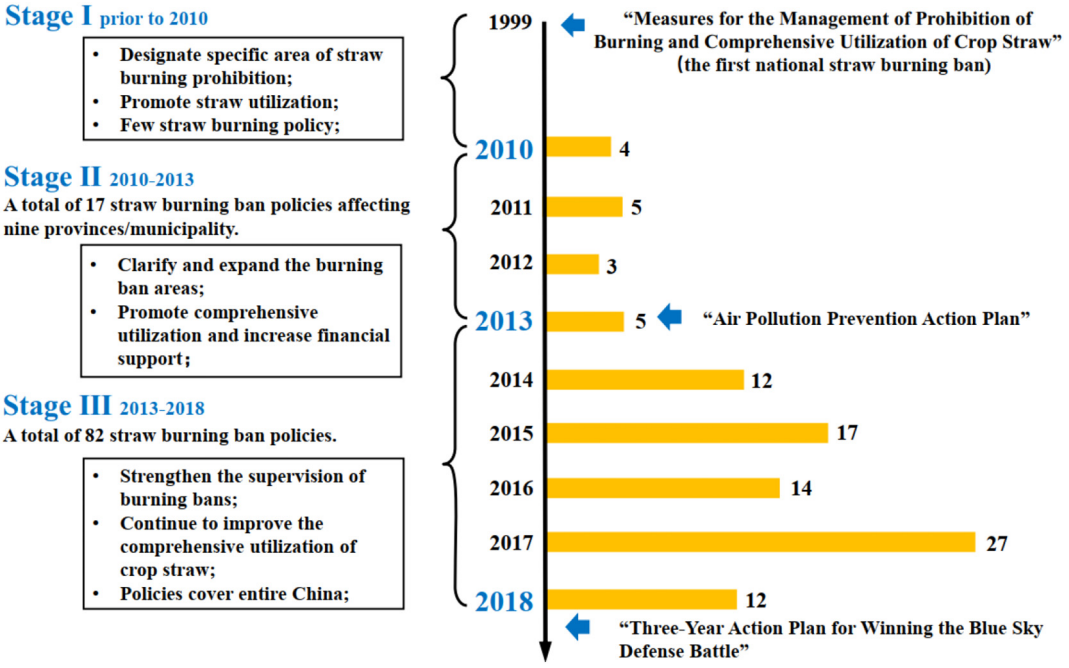

Fig. 1. Timeline of the development of China's control policy related to bans on open crop straw burning and crop straw utilization (numbers next to the bar chart indicates the total number of relevant policies issued this year).

(Stage III), at least 82 relevant policies were issued, affecting 28 provinces in total. Table S1 summarizes a total of 101 relevant policies for straw burning bans at national, regional, and provincial/municipal level that is issued as of 2018. These policies require prohibiting the burning of straw and improving the comprehensive utilization of straw. Among the seven regions, East China has the greatest number of policies (29) while South China has a minimum of 4. In terms of provinces, Shanghai (8) has the most policies related to crop straw burning and straw utilization, followed by the province of Heilongjiang (7), Anhui (6), and Jiangsu (6). In this study, year 2013 is considered as prior to intensive implementation of the straw burning bans and year 2018 as after; the differences between OCSB emissions in 2013 and 2018 are quantified to evaluate the effectiveness of straw burning bans.

2.2. OCSB emissions estimation

The daily Fire INventory from NCAR version 1.5 (FINNv1.5) with a spatial resolution of 1 km was used to characterize the emissions of particles and trace gas from OCSB activities in China during 2010–2018 (Wiedinmyer et al., 2011; https://www.acom.ucar.edu/Data/fire/, accessed on 10th April 2020). Based on satellite fire detection, FINN combines land cover data, emission factors, and fuel loadings to calculate emissions of various air pollutants from burning events in a bottom-up fashion. Land cover data refers to the type of vegetation being burned, which is determined by the MODIS Collection 5 Land Cover Type product for 2005 (Friedl et al., 2010). Emission factors of different air pollutants are collected for different land types based on Akagi et al. (2011), Andreae and Merlet (2001), McMeeking (2008), and Andreae and Rosenfeld (2008). Fuel loadings refers to the amount of available biomass that can be burned in each fire event, which is assigned for different land cover based on values from Hoelzemann et al. (2004). Although uncertainties exist (Wiedinmyer et al., 2011; Chuang et al., 2015; Pimonsree et al., 2018), FINN is commonly used in various studies due to its high spatial and temporal resolution (Mehmood et al., 2018; Uranishi et al., 2019; Mehmood et al., 2020). FINN provides emission estimates for a total of four burning types: forests (tropical, temperate, boreal, temperate evergreen), grasslands and savanna, woody savanna/shrublands, and croplands, of which the last type is the focus of this study. FINN emissions are aggregated to provincial and regional level based on the location of individual fire event. We divided China into seven regions, namely the Northeast China, North China, Central China, East China, South China, Southwest China, and Northwest China, as shown in Fig. 2. Table S2 provides the list of provinces in each region.

2.3. Model configurations

In this study, an integrated meteorology and air quality model is used to quantify the contribution of OCSB emissions to $PM_{2.5}$ concentrations and evaluate the effectiveness of straw burning bans in China. The Weather Research and Forecasting (WRF) model (version 3.4, Skamarock and Klemp, 2008) provides the inputs of meteorological fields and the subsequent air quality is simulated by the latest version of the Comprehensive Air Quality Model with Extension (CAMx, version 7.0, http://www.camx.com/, accessed on 11th January 2020). The configurations in WRF/CAMx are similar to our previous studies (Li et al., 2020; Huang et al., 2021a) and are summarized in Table S3. The modeling domain covers entire China and surrounding countries with a spatial resolution of 36-km (Fig. 2). Anthropogenic emissions for China come from the Multi-resolution Emission Inventory of China for year 2017 (MEIC, http://www.meicmodel.org, accessed on 12th January 2020) developed by Tsinghua University; emissions outside China are based on the European Commission's Emissions Database for Global Atmospheric Research (EDGAR, http://edgar.jrc.ec.europa.eu/index.php, accessed on 14th January 2020) for year 2010. Biogenic emissions are calculated by an updated version of the Model of Emissions of Gases and Aerosols from Nature (MEGAN, version 3.0, http://aqrp.ceer.utexas.edu/projects.cfm, accessed on 15th January 2020). We also calculated sea salt emissions and lightening NO emissions using programs developed by Ramboll (2020) http://www.camx.com/download/support-software.aspx, accessed on 15th January 2020). In addition to the conventional air pollutants, intermediate volatile organic compounds (IVOCs) represent an important precursor of the secondary organic aerosol (SOA) (Robinson et al., 2007; Hodzic et al., 2010; Hayes et al., 2015; Jathar

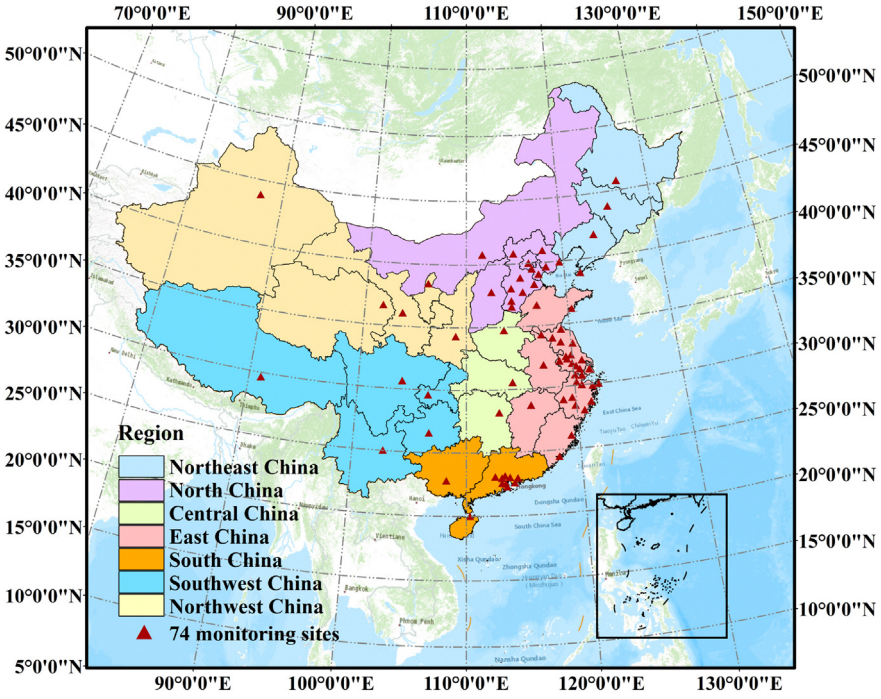

Fig. 2. Map of classified regions and locations of national monitoring sites at 74 major cities.

et al., 2017). However, IVOCs emissions are usually not provided in the traditional emission inventory and only a few studies have studied the IVOCs emissions and its impact of SOA formation in China (Zhao et al., 2016; Wu et al., 2019; Huang et al., 2021a). In this study, we estimated the IVOCs emissions based on the IVOCs-to-primary organic aerosol (POA) ratio method for each emission category; calculation details and source-specific ratios are present in Supplemental Information.

Three simulations were conducted for year 2018 with different OCSB emissions while other model inputs and configurations were kept identical (Table 1). In the base emission scenario, emissions include the base anthropogenic and biogenic emissions and OCSB emissions estimated for 2018. The base case model performance was evaluated using the Pearson correlation coefficient (R), mean bias (MB), root-mean-square error (RMSE), normalized mean bias (NMB), and normalized mean error (NME) against observations. Observed meteorological data, including temperature, wind speed, and relative humidity were obtained from National Meteorological Science Data Center (http://data.cma.cn/). Daily observed concentrations of $PM_{2.5}$, O_3, SO_2, and NO_2 at 74 monitoring sites in China (Fig. 2) were obtained from the China National Environmental Monitoring Center (http://www.cnemc.cn/). Formula for each of the statistical metrics is given in Table S4. In the second scenario, OCSB emissions were excluded and the differences from the base scenarios represent the contribution of OCSB emissions to $PM_{2.5}$ concentrations. In the third scenario, the 2018 OCSB emissions in the base scenario were replaced by the OCSB emissions for year 2013. The differences between the base scenario and the third scenario are used to demonstrate the impacts of straw burning bans on $PM_{2.5}$ concentrations.

Table 1
Simulation scenarios.

Scenario	Emissions except OCSB	OCSB emissions
Scenario 1 (base)	MEIC 2017 + EDGAR 2010 + MEGAN + FINN 2018 for vegetation types except croplands	FINN 2018
Scenario 2		–
Scenario 3		FINN 2013

2.4. Estimation of health impacts

To estimate the health impacts due to long-term $PM_{2.5}$ exposure, the premature mortality due to cerebrovascular disease (stroke), ischemic heart disease (IHD), chronic obstructive pulmonary disease (COPD), and lung cancer (LC) were calculated based on a widely used concentration-response (C-R) model (Burnett et al., 2014):

$$RR(C) = \begin{cases} 1 + \alpha\left(1 - e^{-\gamma(C-C_0)^{\delta}}\right), if\ C > C_0 \\ 1, else \end{cases} \quad (1)$$

$$H = \sum B \times P \times \frac{RR-1}{RR} \quad (2)$$

where RR is the relative risk; C is the simulated annual average $PM_{2.5}$ concentration; C_0 is the threshold value of $PM_{2.5}$ concentration for each disease; α, γ and δ are parameters used to describe the different shapes of the C-R curve among various diseases (Table S5) (Jiang et al., 2015). The national premature mortality (H) attributable to $PM_{2.5}$ were then estimated using Eq. (2) (Xie et al., 2016), in which B is the provincial incidence of a given health impact (https://vizhub.healthdata.org/gbd-compare/, accessed on 16th February 2020) and P is the exposed population of each province in China derived from the 2019 Statistical Yearbook. The number of premature death was first calculated at grid cell level and then aggregated to provincial level. The differences of premature mortality between different scenarios reflect (1) the number of premature mortality associated with OCSB emissions in 2018 and (2) the number of avoided premature mortality as a result of the implementation of straw burning bans.

3. Results and discussions

3.1. Trends of OCSB emissions during 2010–2018

Table 2 summarized the annual emissions of seven air pollutants from OCSB activities averaged during 2010–2018 by province and region. The annual total OCSB emissions of CO, non-methane organic

Table 2
Annual OCSB emissions of major air pollutants by province and region averaged during 2010 to 2018 (unit: Gg/year).

Province	CO	NH_3	NMOC	NOx	PM_{10}	$PM_{2.5}$	SO_2
Northeast China	461.7	13.0	322.9	32.6	39.8	32.9	2.3
Liaoning	60.3	1.6	38.8	3.9	4.8	3.9	0.3
Heilongjiang	332.2	9.3	231.5	23.4	28.5	23.6	1.6
Jilin	69.1	2.1	52.7	5.3	6.5	5.4	0.4
North China	231.0	5.7	140.5	14.2	17.3	14.3	1.0
Hebei	101.9	2.4	59.7	6.0	7.4	6.1	0.4
Inner Mongolia	64.4	1.7	43.0	4.3	5.3	4.4	0.3
Tianjin	15.0	0.4	8.7	0.9	1.1	0.9	0.1
Beijing	13.9	0.3	7.6	0.8	0.9	0.8	0.1
Shanxi	35.8	0.9	21.6	2.2	2.7	2.2	0.2
Central China	265.0	6.3	155.1	15.7	19.1	15.8	1.1
Henan	159.9	3.6	88.7	9.0	10.9	9.0	0.6
Hubei	69.9	1.7	41.9	4.2	5.2	4.3	0.3
Hunan	35.1	1.0	24.5	2.5	3.0	2.5	0.2
East China	710.7	15.8	392.4	39.6	48.3	39.9	2.8
Fujian	15.6	0.4	10.0	1.0	1.2	1.0	0.1
Jiangsu	164.8	3.6	89.5	9.0	11.0	9.1	0.6
Shandong	172.4	3.9	97.2	9.8	12.0	9.9	0.7
Zhejiang	84.3	1.9	45.9	4.6	5.7	4.7	0.3
Shanghai	12.5	0.3	6.6	0.7	0.8	0.7	0.1
Anhui	224.9	4.9	120.8	12.2	14.9	12.3	0.9
Jiangxi	36.2	0.9	22.5	2.3	2.8	2.3	0.2
South China	48.4	1.3	31.1	3.1	3.8	3.2	0.2
Hainan	1.8	0.1	1.3	0.1	0.2	0.1	0.01
Guangdong	32.5	0.8	20.6	2.1	2.5	2.1	0.1
Guangxi	14.1	0.4	9.2	0.9	1.1	0.9	0.1
Southwest China	96.4	2.6	63.2	6.4	7.8	6.4	0.4
Tibet	0.6	0.02	0.4	0.04	0.1	0.04	0.003
Sichuan	45.7	1.1	26.9	2.7	3.3	2.7	0.2
Yunnan	16.5	0.5	12.2	1.2	1.5	1.2	0.1
Chongqing	18.0	0.4	10.8	1.1	1.3	1.1	0.1
Guizhou	15.5	0.5	12.9	1.3	1.6	1.3	0.1
Northwest China	49.6	1.2	28.9	2.9	3.6	2.9	0.2
Xinjiang	19.6	0.5	11.2	1.1	1.4	1.1	0.1
Qinghai	0.9	0.02	0.5	0.1	0.1	0.1	0.004
Gansu	4.2	0.1	2.7	0.3	0.3	0.3	0.02
Ningxia	2.5	0.1	1.6	0.2	0.2	0.2	0.01
Shaanxi	22.4	0.5	12.9	1.3	1.6	1.3	0.1
Total	1862.7	45.7	1134.1	114.5	139.7	115.4	8.0

compounds (NMOC), PM_{10} (aerodynamic diameters less than 10 μm), $PM_{2.5}$, NOx, NH_3, and SO_2 averaged during 2010–2018 were estimated to be 1862.7, 1134.1, 139.7, 115.4, 114.5, 45.7, and 8.0 Gg, respectively. Since the emissions of different air pollutants were linearly correlated with each other, $PM_{2.5}$ is taken as the representative pollutant for further discussions of the temporal and spatial variations. OCSB emissions show significant spatial differences (Fig. 3). Being the main agricultural regions in China, East China and Northeast China (outlined in Fig. 3) are associated with highest $PM_{2.5}$ emissions from OCSB, each accounting for 34.6% and 28.5% of the national total emissions; both high emission intensity (>100 tons/grid cell) and high emission density are observed for these regions. South China and Northwest China exhibit the lowest emissions associated with OCSB, each accounting only 2.7% and 2.5% of the national total. High emission densities are seen over South China but the emission intensities are low (less than 20 tons/grid cell). Heilongjiang, Anhui, Shandong are the top three provinces with highest OCSB $PM_{2.5}$ emissions while Shanghai, Anhui, and Jiangsu show highest emission density (calculated as emissions divided by area).

The year-to-year variations of OCSB emissions during 2010–2018 show substantial regional differences and are illustrated by Fig. 4. The total $PM_{2.5}$ emissions from OCSB exhibit an overall downward trend from 2010 to 2018 with two obvious peaks in 2013 and 2017. The first peak of 152.4 Gg in 2013 is predominantly contributed by emissions from East China (42.5%), Central China (18.1%), Northeast China (14.8%), and North China (13.8%). Except Northeast China, these regions all exhibited an increasing trend from 2010 to 2013 followed by a decreasing trend from 2013 to 2018. In 2018, $PM_{2.5}$ emissions from OSCB activities in these three regions dropped by 74.4%, 64.6%, and 36.1%, respectively, compared to their historical maximum during 2010–2018. In contrast, Northeast China exhibits a completely different trend of OCSB emissions during 2010–2018 with constant increase before 2017 followed by a drastic drop in 2018. OCSB emissions increased from 16.8 Gg in 2010 to 75.6 Gg in 2017, representing a relative increased by 351% (Table S6). The constant increase from 2010 to 2017 reflects the expansion of agricultural sector and economic development in the Northeast China yet relatively unconstrained open burning activities. In 2015, the OCSB emissions in Northeast China exceeded that from East China, becoming the top contributor to national total OCSB emissions for the following years. Therefore, the trend of national total $PM_{2.5}$ emissions from OCSB during 2015–2018 follows Northeast China, where a peak in 2017 followed by a sharp drop in 2018 is observed. OCSB emissions from South China, Northwest China, and Southwest China are comparatively small (together <15% of total emissions) and remains relatively unchanged during 2010–2018.

In terms of the intra-annual variations (Fig. 5), the total $PM_{2.5}$ emissions resulted from OCSB mainly concentrated from March to October due to the harvesting of summer grains and autumn grains (wheat, rice, corn, etc.). These monthly variations also vary by region. For example, in East China, Central China, and North China, peak OCSB activities were observed in June, each accounting for 38.2%, 30.1%, and 17.2% of

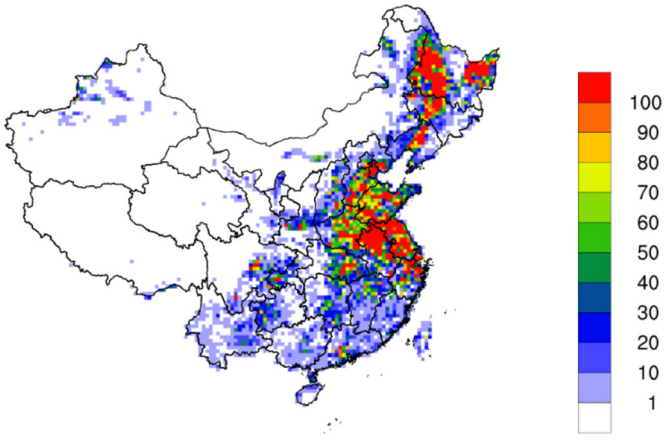

Fig. 3. Spatial distribution of annual $PM_{2.5}$ emissions from OCSB averaged over 2010 to 2018 (unit: tons/grid).

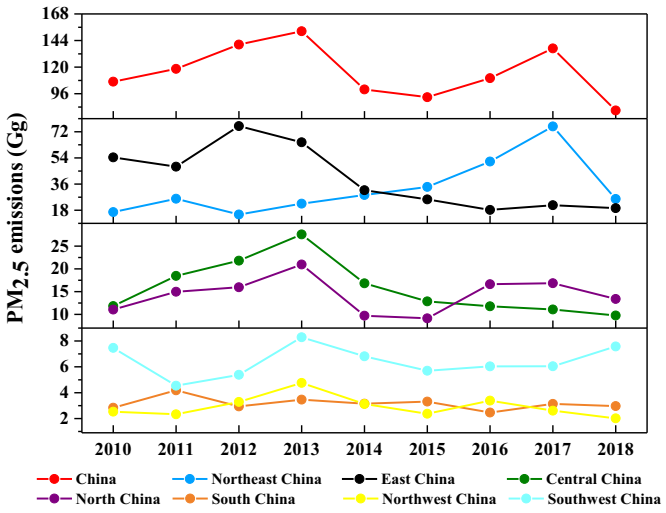

Fig. 4. Emissions of $PM_{2.5}$ from OCSB in China by region from 2010 to 2018.

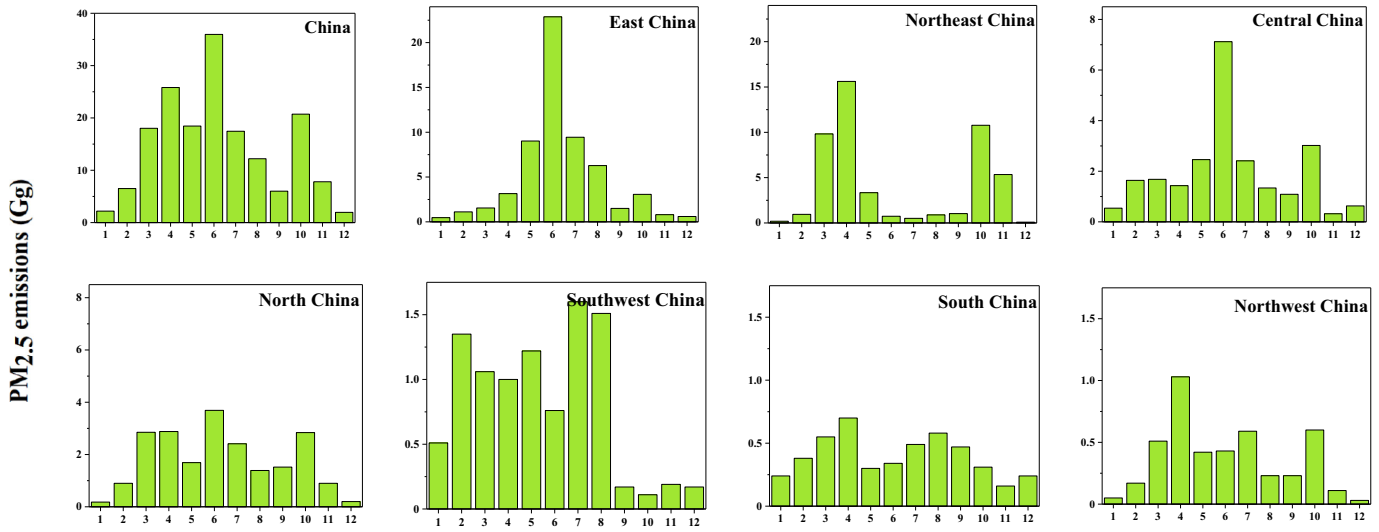

Fig. 5. Monthly $PM_{2.5}$ emissions (unit: Gg) from OCSB by region averaged during 2010–2018.

the annual $PM_{2.5}$ emissions. On the other hand, Northeast China exhibited two distinct peaks of OCSB emissions in April and October while the emissions were negligible during the summer. The monthly variations were mainly associated with the local planting structures and farming habits.

The OCSB emissions based on the FINN dataset is associated with uncertainties (Wiedinmyer et al., 2006; Wiedinmyer et al., 2011). We compared our results with another global fire emission data – the Global Fire Emission Database (with small fires) (GFED4s) as well as results from previous studies (Qiu et al., 2016; Li et al., 2016) for year 2013 (Table 3). Results from Qiu et al. (2016) are mainly based on satellite data while Li et al. (2016) is based on statistical data. In general, the FINN emissions are comparable to that of GFED4s (except for NOx and NMOC, which is much higher with FINN) but were much lower than the other self-developed regional emission estimates (except for NMOC). In terms of $PM_{2.5}$, emissions generated from the global dataset are lower by 85% than regional developed values. Surprisingly, FINN gives the highest estimates of NMOC emissions, probably due to higher emission factors being used. The discrepancies among different emission estimates are mainly associated with the burned area, land-cover characterization, and the emission factors used (Wiedinmyer et al., 2006; Wiedinmyer et al., 2011).

3.2. Impact of OCSB emissions on $PM_{2.5}$ concentrations

3.2.1. Base case evaluation

The performance of the meteorology and air quality modeling system is evaluated to ensure to reasonably reproduce the observed meteorological conditions and air quality levels. Statistical indices used for WRF model evaluation include R, MB, RMSE, NMB, and NME and results are shown in Table S7. Model performances of the base case simulation results for 2018 were evaluated extensively against ground-based observations of daily $PM_{2.5}$, SO_2, NO_2, and O_3 concentrations at 74 national monitoring sites (Fig. 2). Fig. 6 shows the spatial distributions of simulated seasonal averaged $PM_{2.5}$ concentration in 2018 with observation values laid on top. Values of model performance metrics, including MB, RMSE, NMB, NME and R of daily $PM_{2.5}$ concentration by season and region are given in Table 4. Similar results for other pollutants are provided in Fig. S1 and Table S8. As shown in Fig. 6, the model is generally good at capturing the spatial distributions and seasonal variations of the observed $PM_{2.5}$ concentration across China. Underestimation is observed for winter, especially over the North China Plain where highest $PM_{2.5}$ concentrations are observed. The underestimation of $PM_{2.5}$ concentration in winter could be contributed by many factors, of which underestimation of emissions other than OCSB is one of them. Other potential cause of underestimation could be bias in the simulated meteorology, missing formation mechanism for secondary PM species, especially for sulfate and secondary organic aerosols, where underestimations of these species are frequently reported by previous studies (Jiang et al., 2012; Couvidat et al., 2013; Li et al., 2015; Woody et al., 2016; Gao et al., 2016; Meroni et al., 2017; Huang et al., 2019; Huang et al., 2021a). RMSE for different regions ranges 5.8 to 33.4 μg/m^3; R values range from 0.50 to 0.89. Compared with the proposed benchmarks in our previous study (Huang et al., 2021b), most of the calculated statistical metrics were able to meet the "criteria" values, suggesting acceptable model performances. The model is also good at capturing the monthly variations of $PM_{2.5}$ concentrations with underestimation in North China and Northeast China, as shown in Fig. S2. For other pollutants, the model is able to capture the spatial distribution well but overprediction exists for O_3 concentrations while underestimation for NO_2; predicted SO_2 concentration is relatively close to observed values, with an overall MB of 0.1 μg/m^3 and NMB of 1%. In summary, the model performance for the base case scenario is generally acceptable.

Table 3
Comparison of OCSB emissions with previous studies for 2013 (unit: Gg).

Reference	CO	NH_3	NMOC	NOx	$PM_{2.5}$	SO_2
This study	2915	60	1497	151	152	10
GFED	2570	55	249[a]	78	158	10
Qiu et al. (2016)	6098	60	1185	380	1019	52
Li et al. (2016)	7060	140	920	450	1140	70

[a] The NMOC value of GFED is non-methane hydrocarbon (NMHC).

3.2.2. $PM2_{.5}$ concentrations and premature mortality attributable to OCSB

Two simulations with and without OCSB emissions in 2018 (Table 1) were conducted to quantify the contribution of OCSB to $PM_{2.5}$ concentration. Fig. 7a shows the spatial distribution of annual averaged $PM_{2.5}$ concentrations attributable to OCSB emissions. As expected, OCSB emissions lead to ubiquitous increase in $PM_{2.5}$ concentrations across China. Regions with high OCSB emissions, including Northeast China, Central China, and East China, exhibit more impacts with increments of annual averaged $PM_{2.5}$ concentration over 1 μg/m^3 due to open crop burning

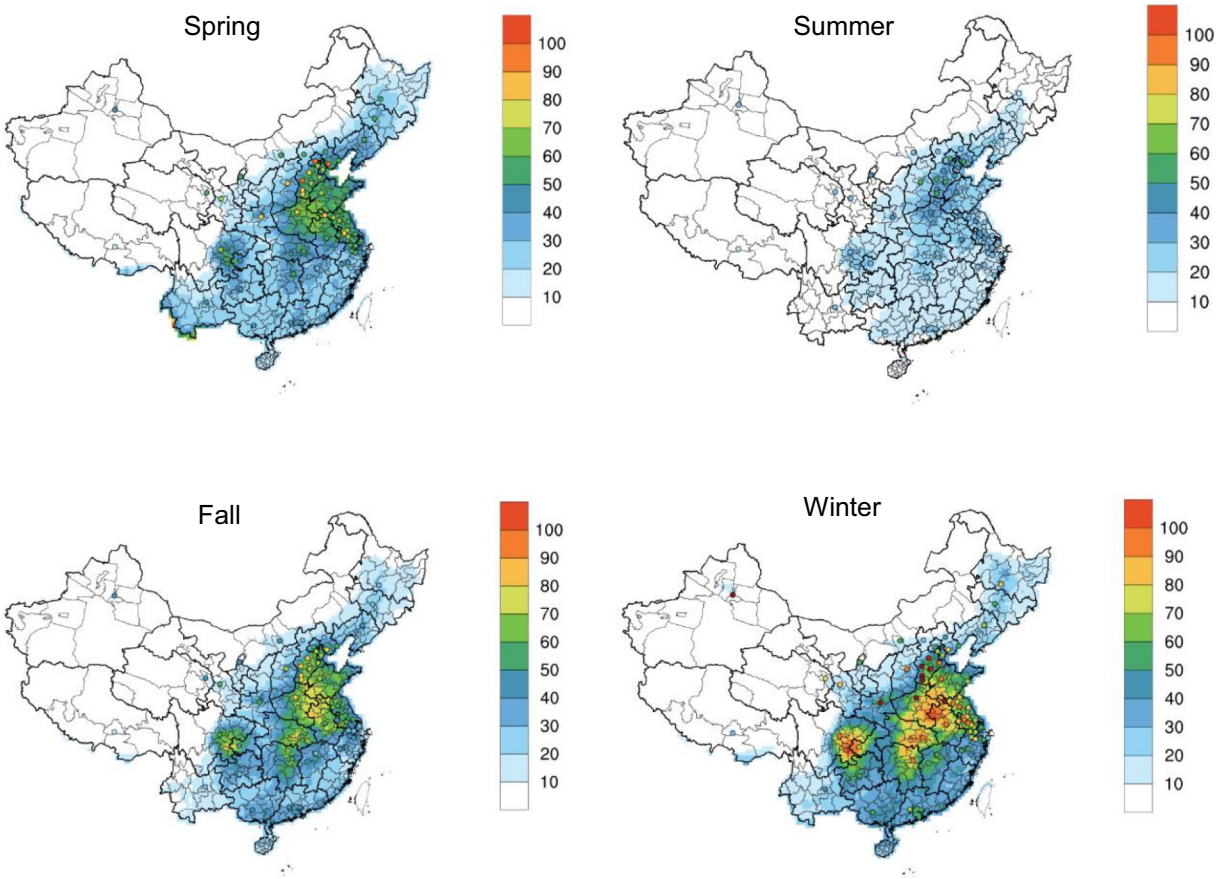

Fig. 6. Spatial distribution of simulated versus observed seasonal average $PM_{2.5}$ concentrations (μg/m^3) in 2018 (observed values shown by dots).

activities. We further looked at the impact of OCSB emissions on $PM_{2.5}$ concentrations by month and by region given that the short-term but intensive feature of OCSB activities. As shown by Fig. 8, the monthly contribution of OCSB activities to $PM_{2.5}$ concentrations mostly correlates to the variations of monthly OCSB emissions but is also affected by the meteorology. For example, Northeast China shows a distinct pattern of the impacts of OCSB emissions on monthly $PM_{2.5}$ concentrations with substantial contributions during February to April and small contribution during other months that match with the monthly variations of OSCB emissions for that region. The maximum increase in monthly average $PM_{2.5}$ concentration could be as much as 10 μg/m^3 in March at certain locations in Northeast China due to the intensive burning activities under unfavorable meteorological conditions. On the other hand, contribution of OCSB activities to $PM_{2.5}$ concentration in East China, North China, and Central China do not exhibit such distinct monthly variations as Northeast China, partly because the OCSB emissions are more evenly spread over multiple months in North China and partly because the relatively favorable meteorological conditions during the summer burning season in East China and Central China offset the negative impacts caused by the OCSB emissions. The $PM_{2.5}$ concentration could be boosted by several μg/m^3 due to OCSB emissions over these regions. OCSB emissions in South China and Northwest China are relatively small compared to the other regions; thus the impacts of OCSB emissions on $PM_{2.5}$ concentrations are correspondingly smaller, with maximum increase of 1.5 μg/m^3 at certain locations.

Table 4
Evaluation of $PM_{2.5}$ concentrations[a].

Region/season	Observed average (μg/m^3)	Simulated average (μg/m^3)	R	MB (μg/m^3)	RMSE (μg/m^3)	NMB	NME
China	41.8	36.2	0.65	−5.5	13.0	−13%	23%
Northeast China	35.7	29.6	**0.50**	−6.1	11.1	−17%	30%
North China	53.7	40.0	0.89	−13.7	15.0	**−26%**	26%
Central China	53.2	56.6	0.87	3.4	6.0	6%	10%
East China	40.0	40.4	0.87	0.5	5.8	1%	11%
South China	30.1	23.7	**0.50**	−6.4	8.0	**−21%**	24%
Southwest China	32.5	38.0	0.88	5.5	15.3	17%	42%
Northwest China	49.9	17.8	0.65	−32.1	33.4	**−64%**	**64%**
Spring	44.6	38.6	0.62	−6.0	13.8	−13%	23%
Summer	26.6	19.5	0.72	−7.1	9.7	**−27%**	31%
Fall	38.0	41.0	0.70	3.0	13.5	8%	27%
Winter	58.6	46.3	**0.51**	−12.3	24.8	**−21%**	28%

[a] Bolded values indicate that our value fail to meet the "criteria" values in Huang et al. (2021b).

In the base scenario, the number of total premature deaths caused by $PM_{2.5}$ exposure in China in 2018 was estimated to be 967,230 (see detailed number in Table S9), which is similar to results from other studies (e.g. Ding et al., 2019; Wang et al., 2020). Stroke, IHD, COPD, and LC each contributed 50.7%, 29.9%, 10.3% and 9.1% of the total premature mortality, respectively. The spatial distribution of premature mortality due to $PM_{2.5}$ exposure (Fig. S3) coincides with the region with both high population density and high $PM_{2.5}$ concentrations. The top five provinces that have highest premature mortality due to $PM_{2.5}$ exposure are Shandong (99,772), Henan (85,756), Sichuan (78,216), Jiangsu (74,234), and Hebei (69,354). The number of premature deaths associated with OCSB activities was estimated to be 4741 in 2018, accounting for 0.49% of the total deaths. Spatially (Fig. 7c), health impacts from OCSB were mainly concentrated in the areas where OCSB emissions were high, for example, East China (1434) and Northeast China (1004). The five provinces that exhibit highest premature mortality due to OCSB in 2018 were

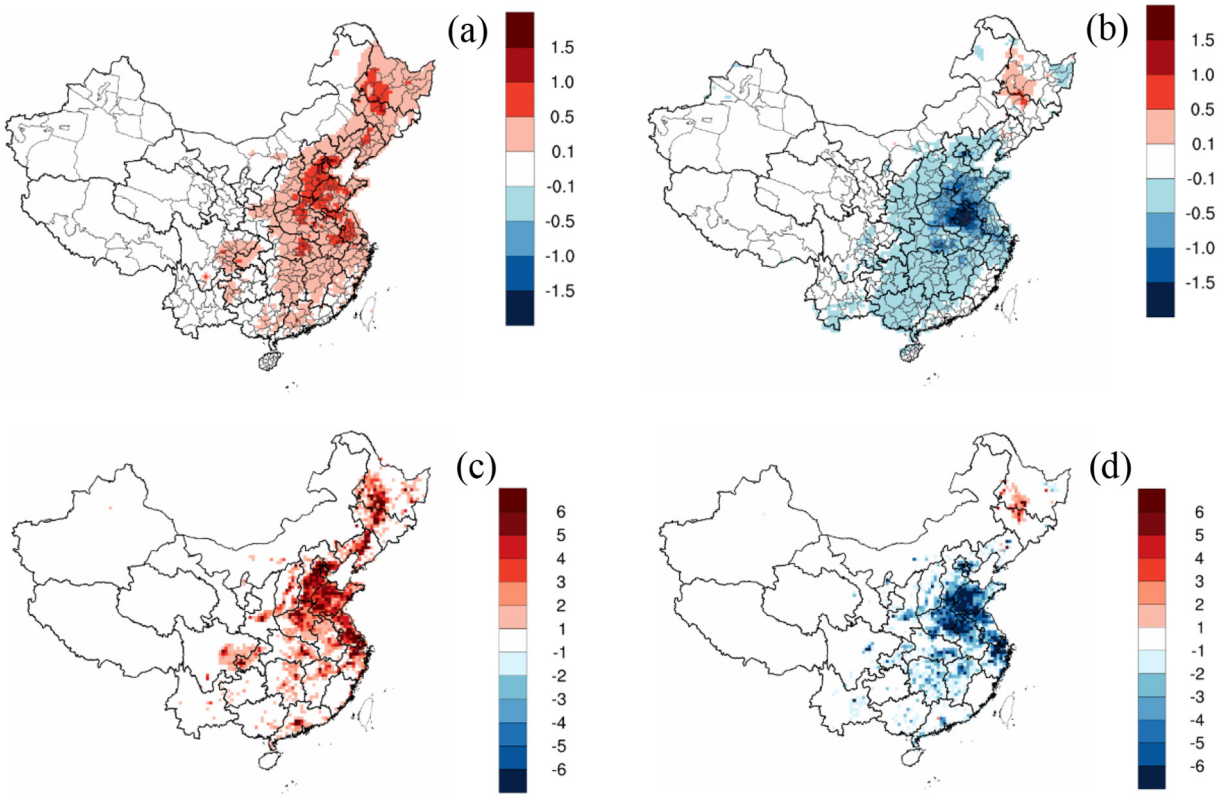

Fig. 7. Spatial distribution of changes in annual $PM_{2.5}$ concentration (unit: μg/m^3; upper row) and premature mortality (unit: person/grid; bottom row) due to OCSB emissions (left) and straw burning bans (right) (No data for Taiwan, Hong Kong and Macau).

Hebei (517), Heilongjiang (481), Shandong (445), Jiangsu (337) and Henan (319), which together accounted for 44.3% of the total premature deaths attributable to OCSB.

3.3. Impact of straw burning bans

3.3.1. Changes in OCSB emissions

To mitigate the severe haze pollution in China, the central and local governments have strengthened the prohibition of open straw burning and promoted the financial support for straw utilization in the past few years. Since 2013, the number of policies related to straw burning bans has grown exponentially (Fig. 1). Here we consider year 2013 as prior to the implementation of intensive straw burning bans and year 2018 when banning policies reached their strictest level. The total $PM_{2.5}$ emissions associated with OSCB are estimated to be 80.9 Gg in 2018, representing an absolute reduction by 71.4 Gg and a relative reduction by 46.9% from 2013. Reductions of OCSB emissions in 2018 are prominent during May to October (Fig. 9), with maximum absolute decrease

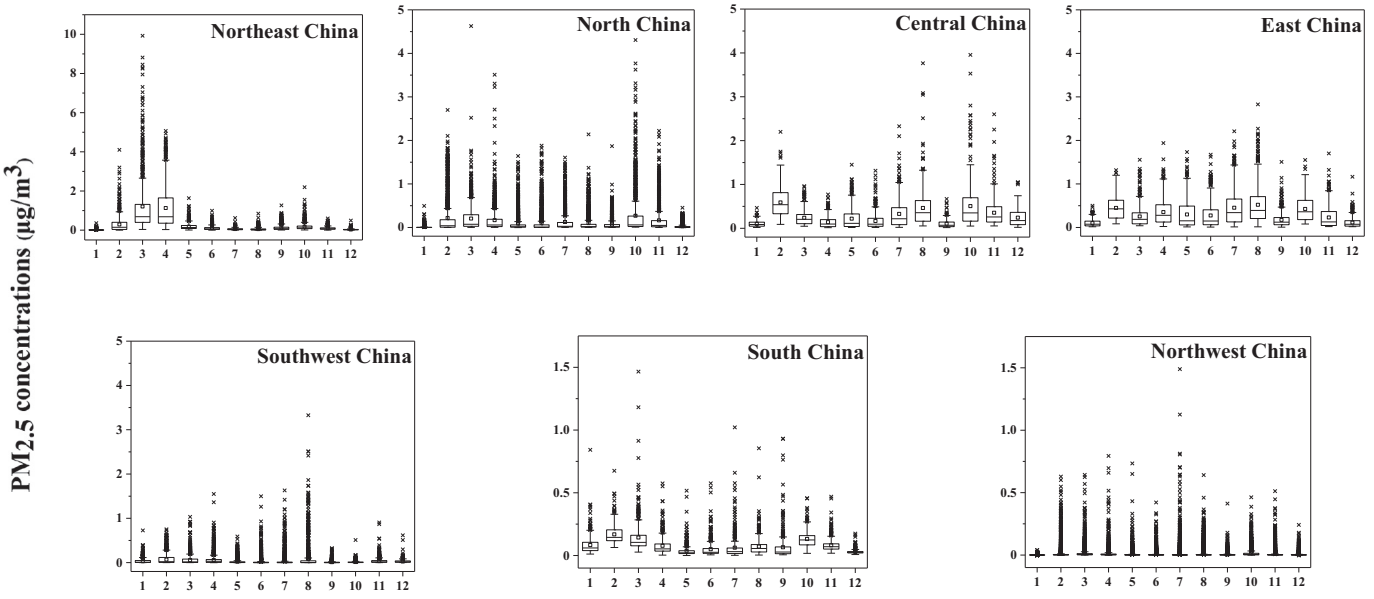

Fig. 8. Monthly averaged $PM_{2.5}$ concentrations (μg/m^3) due to OCSB by month and region.

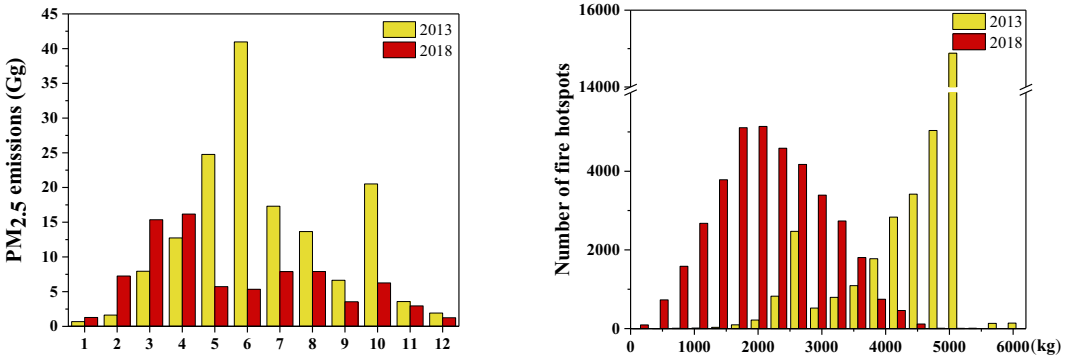

Fig. 9. Comparison of national total $PM_{2.5}$ emissions (left) and number of OCSB fires grouped by $PM_{2.5}$ emissions (right) in 2013 and 2018.

of 35.6 Gg and maximum relative decrease of 87% in June. However, increase in $PM_{2.5}$ emissions by 27%–340% were observed for January–April of 2018. In February, $PM_{2.5}$ emissions caused by OCSB activities increased by 4 times in 2018 compared to 2013. These monthly changes of the national total $PM_{2.5}$ emissions are contributed by changes in OCSB activities for different regions. For example, East China, North China, and Central China show high OCSB emissions during late spring and summer months (Fig. 5); meanwhile, these regions show significant decrease of OCSB emissions in 2018 (70% for East China, 36% for North China, and 65% for Central China) as a result of the implementation of straw burning bans (Fig. S4); therefore, the national total $PM_{2.5}$ emissions during May to October dropped substantially in 2018. Provinces located in East China and Central China, for example, Jiangsu, Shandong, and Anhui, all exhibit significant reductions in open crop burning activities and associated $PM_{2.5}$ emissions since 2013. In contrast, Northeast China is the only region that show increased OCSB activities (number of fire events increased by 105.8%) and associated $PM_{2.5}$ emissions (by 14%) in 2018 compared to 2013. As mentioned above, OCSB activities in Northeast China increased consistently during 2013–2017; although a drastic drop occurred in 2018 compared to the maximum in 2017, emissions of $PM_{2.5}$ and other pollutants in 2018 are still higher than the amount in 2013, especially during February – April (Fig. S5), therefore leading to increased emissions during these months. This reflects a delayed implementation of prohibitions on open burning activities in Northeast China compared to other parts of China. Emissions in other regions (South China, Southwest China, and Northwest China) all show reductions by 8% ~ 58% in 2018; however, because their emissions are relatively small thus do not have much impacts on the overall changes.

We further compared the characteristics of OCSB activities before and after the implementation of straw burning bans by grouping OCSB events based on the $PM_{2.5}$ emissions into bins of 10^3 kg (Fig. 9). In 2013, crop burning activities were dominated by burning events with relatively large emissions (>4000 kg per event), suggesting either large burned areas or long burning period. In 2018, crop burning activities shifted towards small burning events with higher frequency of fires but with much lower emissions (<2500 kg per event). Different regions have similar changes (Fig. S6). These changes imply that the straw burning bans are more effective at reducing large fire events but more efforts may be needed to control small fire events.

3.3.2. Impact on $PM_{2.5}$ concentrations and premature death

To evaluate the effectiveness of the burning bans on regional air quality, we replaced the 2018 OCSB emissions in the base case scenario with 2013 emissions while keeping other emissions and model configurations unchanged. The differences in simulated $PM_{2.5}$ concentrations are solely attributable to changes in OCSB emissions. As shown in Fig. 7b, simulated annual averaged $PM_{2.5}$ concentrations show widespread reductions over China as a result of changes in OCSB emissions; reductions are prominent in East China and maximum decrease exceed 2.0 μg/m^3. Fig. 10 shows the absolute changes of monthly average $PM_{2.5}$ concentration by grid cells for each region and month. It should be note that the locations of OCSB activities do not always match in space

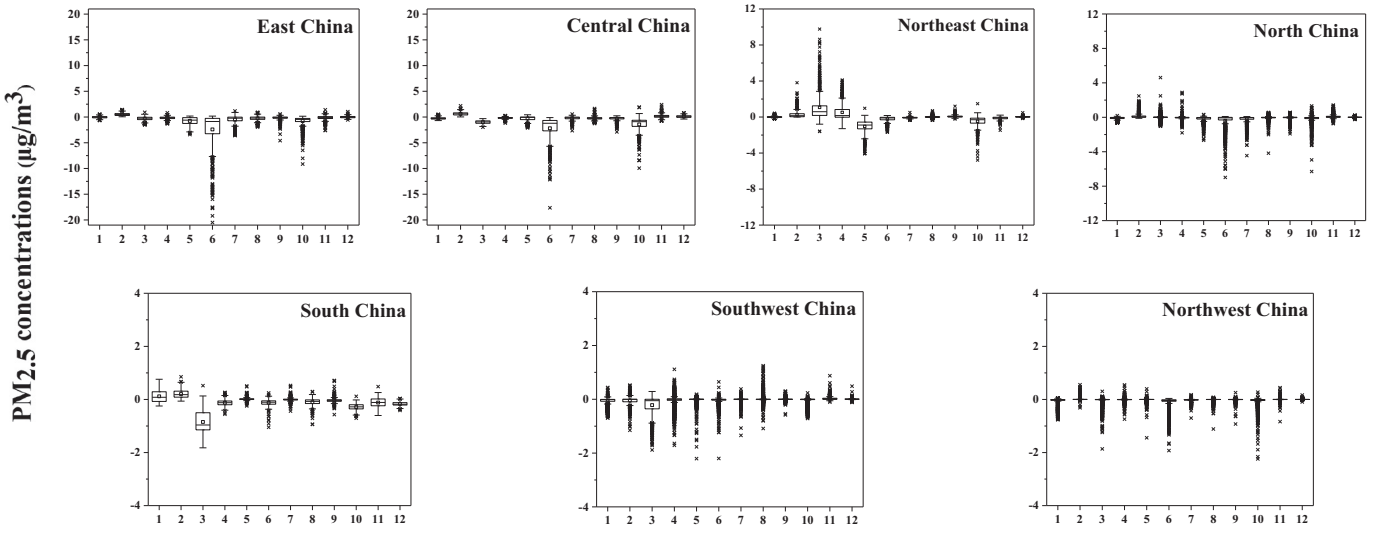

Fig. 10. Change of monthly averaged $PM_{2.5}$ concentration due to OCSB emission changes between 2013 and 2018 by region and month.

between 2013 and 2018 thus increases of $PM_{2.5}$ concentration exist for certain grid cells. All regions (except Northeast China) show an overall trend of reductions in monthly average $PM_{2.5}$ concentrations and follow the pattern of changes in monthly OCSB emissions. For example, great reductions in monthly averaged $PM_{2.5}$ concentration were observed for June in East China with an averaged decrease by 2.4 μg/m^3 and maximum decrease exceeding 20 μg/m^3 at certain locations. The corresponding OCSB emissions decreased by 92% in June 2018 compared to June 2013. Monthly averaged $PM_{2.5}$ concentration in June and October of North China also exhibit substantial reductions that correspond to huge reductions of OCSB emissions from 2013 to 2018 for these two months (66% and 32% for June and October). Northeast China exhibit increases of monthly $PM_{2.5}$ concentrations during the burning seasons because OCSB emissions during 2018 are still higher than 2013; on average, the $PM_{2.5}$ concentration increased by 1.1 μg/m^3 in March with maximum increase of 9.8 μg/m^3.

The total number of premature deaths associated with $PM_{2.5}$ exposure was estimated to be 971,486 if the OCSB emissions were kept at 2013 level. Therefore, the total number of avoided premature deaths due to reductions of OCSB emissions was estimated to be 4256 and the spatial distribution mimics the changes in simulated changes in $PM_{2.5}$ concentration (Fig. 7d). East China had the highest number of avoided premature mortality of 1958, accounting for 46.0% of the total avoided deaths, followed by Central China (907), and North China (634). The top five provinces with the highest number of avoided premature deaths due to the implementation of straw burning bans were Shandong (522), Henan (476), Anhui (449), Jiangsu (358) and Hebei (314). Because emissions from crop burning activities in Northeast China increased slightly in 2018, the number of premature deaths actually shows an increase of 83. The results demonstrated that even greater number of saved lives can be achieved by further reducing OCSB emissions.

4. Conclusions

Being a common agricultural practice in China, open crop straw burning represents an important source of atmospheric pollutants. Based on the FINN inventory, high OCSB emissions concentrated over Northeast China (31.8% of national total $PM_{2.5}$ emissions in 2018), East China (24.0%), and North China (16.6%). Spatial heterogeneities were found with both the monthly and inter-annual variations of OCSB emissions. Northeast China shows two peaks of OCSB emissions in April and October while emissions in East China and Central China are intense during the summer. An overall decrease of annual OCSB emissions are observed in East China, Central China, and North China since 2013 whereas Northeast China exhibits peak emissions in 2017 followed by a dramatic drop in 2018. Simulation results show that OCSB emissions could increase the annual $PM_{2.5}$ concentration by as 1 μg/m^3 in Northeast China, East China, and Central China; maximum increase in monthly $PM_{2.5}$ concentration could be as high as 10 μg/m^3 in Northeast China. In 2018, OCSB emissions are associated with a total number of 4741 premature deaths due to long-term $PM_{2.5}$ exposure.

To mitigate the air pollution problem, series of policies related to the prohibition of crop straw burning in the open fields were formulated and implemented at different levels and over different regions of China during the past years. The national total $PM_{2.5}$ emissions from OCSB activities in 2018 dropped by 46.9% compared to the values in 2013, a year considered as the beginning of intensive implementation of straw burning bans. Significant decreases of OCSB emissions were found in East China (70%), Central China (65%), and Northwest China (58%). Total avoided premature deaths are estimated to be 4256 due to reduced OCSB emissions; Shandong (522), Henan (476) and Anhui (449) represent the top three provinces that gained most health benefits. However, although the implementation of straw burning bans leads to sharp decrease of OCSB emissions in Northeast China from 2017 to 2018, the OCSB emissions in 2018 were still higher than 2013. Results from this study demonstrate the spatial heterogeneities in terms of the effectiveness of straw burning bans on reducing $PM_{2.5}$ concentrations and associated health impacts and even greater number of saved lives can be achieved by further reducing OCSB emissions.

CRediT authorship contribution statement

Ling Huang: Methodology, Investigation, Formal analysis, Writing – review & editing. **Yonghui Zhu:** Methodology, Investigation, Formal analysis, Writing – original draft. **Qian Wang:** Formal analysis. **Ansheng Zhu:** Formal analysis. **Ziyi Liu:** Formal analysis. **Yangjun Wang:** Formal analysis. **David T. Allen:** Writing – review & editing. **Li Li:** Conceptualization, Methodology, Writing – review & editing, Funding acquisition.

Declaration of competing interest

The authors declare that they have no known competing financial interests or personal relationships that could have appeared to influence the work reported in this paper.

Acknowledgement

This study was financially sponsored by the National Natural Science Foundation of China (grant no. 42005112), the Shanghai Science and Technology Innovation Plan (no. 19DZ1205007), the Shanghai Sail Program (no. 19YF1415600), the National Natural Science Foundation of China (nos. 42075144, 41875161), the Shanghai International Science and Technology Cooperation Fund (no. 19230742500), and Chinese National Key Technology R&D Program (no. 2018YFC0213800).

Appendix A. Supplementary data

Supplementary data to this article can be found online at https://doi.org/10.1016/j.scitotenv.2021.147935.

References

Akagi, S.K., Yokelson, R.J., Wiedinmyer, C., Alvarado, M.J., Reid, J.S., Karl, T., Crounse, J.D., Wennberg, P.O., 2011. Emission factors for open and domestic biomass burning for use in atmospheric models. Atmos. Chem. Phys. 11, 4039–4072. https://doi.org/10.5194/acp-11-4039-2011.

Andreae, M.O., Merlet, P., 2001. Emission of trace gases and aerosols from biomass burning. Glob. Biogeochem. Cycles 15 (4), 955–966. https://doi.org/10.1029/2000GB001382.

Andreae, M.O., Rosenfeld, D., 2008. Aerosol-cloudprecipitation interactions. Part 1, the nature and sources of cloud-active aerosols. Earth Sci. Rev. 89, 13–41 doi:j.earscirev.2008.03.001.

Bei, N.F., Li, X.P., Tie, X.X., Zhao, L.N., Wu, J.R., Li, X., Liu, L., Shen, Z.X., Li, G.H., 2020. Impact of synoptic patterns and meteorological elements on the wintertime haze in the Beijing-Tianjin-Hebei region, China from 2013 to 2017. Sci. Total Environ. 704, 135210. https://doi.org/10.1016/j.scitotenv.2019.135210.

Bond, T.C., Streets, D.G., Yarber, K.F., Nelson, S.M., Woo, J.-H., Klimont, Z., 2004. A technology-based global inventory of black and organic carbon emissions from combustion. J. Geophys. Res. 109, D14203. https://doi.org/10.1029/2003JD003697.

Burnett, R.T., Pope, C.A., Ezzati, M., Olives, C., Lim, S.S., Mehta, S., Shin, H.H., Singh, G., Hubbell, B., Brauer, M., Anderson, H.R., Smith, K.R., Balmes, J.R., Bruce, N.G., Kan, H., Laden, F., Pruss-Ustun, A., Turner, M.C., Gapstur, S.M., Diver, W.R., Cohen, A., 2014. An integrated risk function for estimating the global burden of disease attributable to ambient fine particulate matter exposure. Environ. Health Perspect. 122 (4), 397–403. https://doi.org/10.1289/ehp.1307049.

Cheng, Z., Wang, S., Fu, X., Watson, J.G., Jiang, J., Fu, Q., Chen, C., Xu, B., Yu, J., Chow, J.C., Hao, J., 2014. Impact of biomass burning on haze pollution in the Yangtze River delta, China: a case study in summer 2011. Atmos. Chem. Phys. 14 (9), 4573–4585. https://doi.org/10.5194/acp-14-4573-2014.

Chuang, M.T., Fu, J.S., Lin, N.H., Lee, C.T., Gao, Y., Wang, S.H., Sheu, G.R., Hsiao, T.C., Wang, J.L., Yen, M.C., Lin, T.H., Thongboonchoo, N., Chen, W.C., 2015. Simulating the transport and chemical evolution of biomass burning pollutants originating from Southeast Asia during 7-SEAS/2010 Dongsha experiment. Atmos. Environ. 112, 294–305. https://doi.org/10.1016/j.atmosenv.2015.04.055.

Couvidat, F., Kim, Y., Sartelet, K., Seigneur, C., Marchand, N., Sciare, J., 2013. Modeling secondary organic aerosol in an urban area: application to Paris, France. Atmos. Chem. Phys. 13 (2), 983–996. https://doi.org/10.5194/acp-13-983-2013.

Ding, D., Xing, J., Wang, S., Liu, K., Hao, J., 2019. Estimated contributions of emissions controls, meteorological factors, population growth, and changes in baseline mortality to

reductions in ambient $PM_{2.5}$ and $PM_{2.5}$-related mortality in China, 2013–2017. Environ. Health Perspect. 127 (6), 067009. https://doi.org/10.1289/ehp4157.
Friedl, M.A., Sulla-Menashe, D., Tan, B., Schneider, A., Ramankutty, N., Sibley, A., Huang, X., 2010. MODIS collection 5 global land cover: algorithm refinements and characterization of new datasets. Remote Sens. Environ. 114 (1), 168–182. https://doi.org/10.1016/j.rse.2009.08.016.
Gadde, B., Bonnet, S., Menke, C., Garivait, S., 2009. Air pollutant emissions from rice straw open field burning in India, Thailand and the Philippines. Environ. Pollut. 157 (5), 1554–1558. https://doi.org/10.1016/j.envpol.2009.01.004.
Gao, M., Carmichael, G.R., Wang, Y., Ji, D., Liu, Z., Wang, Z., 2016. Improving simulations of sulfate aerosols during winter haze over Northern China: the impacts of heterogeneous oxidation by NO_2. Front. Environ. Sci. Eng. 10 (5), 1–11. https://doi.org/10.1007/s11783-016-0878-2.
Gao, L.B., Wang, T.J., Ren, X.J., Zhuang, B.L., Li, S., Yao, R., Yang, X.Q., 2020. Impact of atmospheric quasi-biweekly oscillation on the persistent heavy $PM_{2.5}$ pollution over Beijing-Tianjin-Hebei region, China during winter. Atmos. Res. 242, 105017. https://doi.org/10.1016/j.atmosres.2020.105017.
Hayes, P.L., Carlton, A.G., Baker, K.R., Ahmadov, R., Washenfelder, R.A., Alvarez, S., Rappenglück, B., Gilman, J.B., Kuster, W.C., de Gouw, J.A., Zotter, P., Prévôt, A.S.H., Szidat, S., Kleindienst, T.E., Offenberg, J.H., Ma, P.K., Jimenez, J.L., 2015. Modeling the formation and aging of secondary organic aerosols in Los Angeles during CalNex 2010. Atmos. Chem. Phys. 15 (10), 5773–5801. https://doi.org/10.5194/acp-15-5773-2015.
Hodzic, A., Jimenez, J.L., Madronich, S., Canagaratna, M.R., DeCarlo, P.F., Kleinman, L., Fast, J., 2010. Modeling organic aerosols in a megacity: potential contribution of semi-volatile and intermediate volatility primary organic compounds to secondary organic aerosol formation. Atmos. Chem. Phys. 10 (12), 5491–5514. https://doi.org/10.5194/acp-10-5491-2010.
Hoelzemann, J.J., Schultz, M.G., Brasseur, G.P., Granier, C., Simon, M., 2004. Global Wildland Fire Emission Model (GWEM): evaluating the use of global area burnt satellite data. J. Geophys. Res. 109, D14S04. https://doi.org/10.1029/2003JD003666.
Hong, J., Ren, L., Hong, J., Xu, C., 2016. Environmental impact assessment of corn straw utilization in China. J. Clean. Prod. 112, 1700–1708. https://doi.org/10.1016/j.jclepro.2015.02.081.
Huang, L., An, J., Koo, B., Yarwood, G., Yan, R., Wang, Y., Huang, C., Li, L., 2019. Sulfate formation during heavy winter haze events and the potential contribution from heterogeneous SO_2+ NO_2 reactions in the Yangtze River Delta region, China. Atmos. Chem. Phys. 19 (22), 14311–14328. https://doi.org/10.5194/acp-19-14311-2019.
Huang, L., Wang, Q., Wang, Y.J., Emery, C., Zhu, A.S., Zhu, Y.H., Yin, S.J., Yarwood, G., Zhang, K., Li, L., 2021a. Simulation of secondary organic aerosol over the Yangtze River Delta region: the impacts from the emissions of intermediate volatility organic compounds and the SOA modeling framework. Atmos. Environ. 246, 118079. https://doi.org/10.1016/j.atmosenv.2020.118079.
Huang, L., Zhu, Y.H., Zhai, H.H., Xue, S.H., Zhu, T.Y., Shao, Y., Liu, Z.Y., Emery, C., Yarwood, G., Wang, Y.J., Fu, J.S., Zhang, K., Li, L., 2021b. Recommendations on benchmarks for numerical air quality model applications in China: part I – $PM_{2.5}$ and chemical species. Atmos. Chem. Phys. 21, 2725–2743. https://doi.org/10.5194/acp-21-2725-2021.
Jathar, S.H., Woody, M., Pye, H.O.T., Baker, K.R., Robinson, A.L., 2017. Chemical transport model simulations of organic aerosol in southern California: model evaluation and gasoline and diesel source contributions. Atmos. Chem. Phys. 17 (6), 4305–4318. https://doi.org/10.5194/acp-17-4305-2017.
Jiang, F., Liu, Q., Huang, X., Wang, T., Zhuang, B., Xie, M., 2012. Regional modeling of secondary organic aerosol over China using WRF/Chem. J. Aerosol Sci. 43 (1), 57–73. https://doi.org/10.1016/j.jaerosci.2011.09.003.
Jiang, X., Zhang, Q., Zhao, H., Geng, G., Peng, L., Guan, D., Kan, H., Huo, H., Lin, J., Brauer, M., Martin, R.V., He, K., 2015. Revealing the hidden health costs embodied in Chinese exports. Environ. Sci. Technol. 49 (7), 4381–4388. https://doi.org/10.1021/es506121s.
Junpen, A., Pansuk, J., Kamnoet, O., Cheewaphongphan, P., Garivait, S., 2018. Emission of air pollutants from rice residue open burning in Thailand, 2018. Atmosphere 9 (11), 449. https://doi.org/10.3390/atmos9110449.
Korontzi, S., McCarty, J., Loboda, T., Kumar, S., Justice, C., 2006. Global distribution of agricultural fires in croplands from 3 years of Moderate Resolution Imaging Spectroradiometer (MODIS) data. Glob. Biogeochem. Cycles 20, GB2021. https://doi.org/10.1029/2005GB002529.
Kumar, P., Kumar, S., Joshi, L., 2015. Socioeconomic and Environmental Implications of Agricultural Residue Burning: A Case Study of Punjab, India. Springer Nature, p. 144 https://doi.org/10.1007/978-81-322-2014-5.
Li, M., Zhang, L.L., 2014. Haze in China: current and future challenges. Environ. Pollut. 189, 85–86. https://doi.org/10.1016/j.envpol.2014.02.024.
Li, L., An, J.Y., Zhou, M., Yan, R.S., Huang, C., Lu, Q., Lin, L., Wang, Y.J., Tao, S.K., Qiao, L.P., Zhu, S.H., Chen, C.H., 2015. Source apportionment of fine particles and its chemical components over the Yangtze River Delta, China during a heavy haze pollution episode. Atmos. Environ. 123, 415–429. https://doi.org/10.1016/j.atmosenv.2015.06.051.
Li, J., Li, Y., Bo, Y., Xie, S., 2016. High-resolution historical emission inventories of crop residue burning in fields in China for the period 1990–2013. Atmos. Environ. 138, 152–161. https://doi.org/10.1016/j.atmosenv.2016.05.002.
Li, L., Li, Q., Huang, L., Wang, Q., Zhu, A.S., Xu, J., Liu, Z.Y., Li, H.L., Shi, L.S., Li, R., Azari, M., Wang, Y.J., Zhang, X.J., Liu, Z.Q., Zhu, Y.H., Zhang, K., Xue, S.H., Ooi, M.C.G., Zhang, D.P., Chan, A., 2020. Air quality changes during the COVID-19 lockdown over the Yangtze River Delta Region: an insight into the impact of human activity pattern changes on air pollution variation. Sci. Total Environ. 732, 139282. https://doi.org/10.1016/j.scitotenv.2020.139282.
McMeeking, G.R., 2008. The Optical, Chemical, and Physical Properties of Aerosols and Gases Emitted by the Laboratory Combustion of Wildland Fuels. Ph.D. Dissertation. Department of Atmospheric Sciences, Colorado State University, pp. 109–113.
Mehmood, K., Chang, S., Yu, S., Wang, L., Li, P., Li, Z., Liu, W., Rosenfeld, D., Seinfeld, J.H., 2018. Spatial and temporal distributions of air pollutant emissions from open crop straw and biomass burnings in China from 2002 to 2016. Environ. Chem. Lett. 16 (1), 301–309. https://doi.org/10.1007/s10311-017-0675-6.
Mehmood, K., Wu, Y.J., Wang, L.J., Yu, S.C., Li, P.F., Chen, X., Li, Z., Zhang, Y.B., Li, M.Y., Liu, W.P., Wang, Y.S., Liu, Z.R., Zhu, Y.N., Rosenfeld, D., Seinfeld, J.H., 2020. Relative effects of open biomass burning and open crop straw burning on haze formation over central and eastern China: modeling study driven by constrained emissions. Atmos. Chem. Phys. 20, 244–2419. https://doi.org/10.5194/acp-20-2419-2020.
Meroni, A., Pirovano, G., Gilardoni, S., Lonati, G., Colombi, C., Gianelle, V., Paglione, M., Poluzzi, V., Riva, G.M., Toppetti, A., 2017. Investigating the role of chemical and physical processes on organic aerosol modelling with CAMx in the Po Valley during a winter episode. Atmos. Environ. 171, 126–142. https://doi.org/10.1016/j.atmosenv.2017.10.004.
Pandey, P., Valkenburg, G., Mamidipudi, A., Bijker, W.E., 2017. The Key to Resolving Straw Burning: farmers' Expertise. Policy Brief on Missing Cultural Perspectives. Maastricht University, Maastricht, the Netherlands.
Pimonsree, S., Vongruang, P., Sumitsawan, S., 2018. Modifified biomass burning emission in modeling system with fifire radiative power: simulation of particulate matter in Mainland Southeast Asia during smog episode. Atmos. Pollut. Res. 9, 133–145. https://doi.org/10.1016/j.apr.2017.08.002.
Pollution Control Department (PCD), 2012. Pollution Control Plan 2012–2016. Pollution Control Department, Bangkok, Thailand, p. 38 Available online: http://infofile.pcd.go.th/mgt/Pcd_plan55to59.pdf.
Qiu, X., Duan, L., Chai, F., Wang, S., Yu, Q., Wang, S., 2016. Deriving high-resolution emission inventory of open biomass burning in China based on satellite observations. Environ. Sci. Technol. 50 (21), 11779–11786. https://doi.org/10.1021/acs.est.6b02705.
Ramboll, 2020. CAMx (Comprehensive Air Quality Model With Extensions) User's Guide. Version 7.0. www.camx.com.
Robinson, A.L., Donahue, N.M., Shrivastava, M.K., Weitkamp, E.A., Sage, A.M., Grieshop, A.P., Lane, T.E., Pierce, J.R., Pandis, S.N., 2007. Rethinking organic aerosols: semivolatile emissions and photochemical aging. Science 315, 1259–1262. https://doi.org/10.1126/science.1133061.
Seglah, P.A., Wang, Y., Wang, H., Bi, Y., Zhou, K., Wang, Y., Wang, H., Feng, X., 2020. Crop straw utilization and field burning in Northern region of Ghana. J. Clean. Prod. 261, 121191. https://doi.org/10.1016/j.jclepro.2020.121191.
Shen, J.Y., Zhao, Q.B., Cheng, Z., Huo, J.T., Zhu, W.F., Zhang, Y.H., Duan, Y.S., Wang, X.L., Chen, L.W.A., Fu, Q.Y., 2020. Evolution of source contributions during heavy fine particulate matter ($PM_{2.5}$) pollution episodes in eastern China through online measurements. Atmos. Environ. 232, 117569. https://doi.org/10.1016/j.atmosenv.2020.117569.
Skamarock, W.C., Klemp, J.B., 2008. A time-split nonhydrostatic atmospheric model for weather research and forecasting applications. J. Comput. Phys. 227, 2485–3465. https://doi.org/10.1016/j.jcp.2007.01.037.
Streets, D.G., Bond, T.C., Carmichael, G.R., Fernandes, S.D., Fu, Q., He, D., Klimont, Z., Nelson, S.M., Tsai, N.Y., Wang, M.Q., Woo, J.H., Yarber, K.F., 2003. An inventory of gaseous and primary aerosol emissions in Asia in the year 2000. J. Geophys. Res. Atmos. 108 (D21), 8809. https://doi.org/10.1029/2002JD003093.
Sun, D.Q., Ge, Y., Zhou, Y.H., 2019. Punishing and rewarding: how do policy measures affect crop straw use by farmers? An empirical analysis of Jiangsu Province of China. Energy Policy 134, 110882. https://doi.org/10.1016/j.enpol.2019.110882.
Tore, A., 2019. Thinking Glocal to solve India's paddy-straw burning crisis. Agriculture News in Down To Earth.
Uranishi, K., Ikemori, F., Shimadera, H., Kondo, A., Sugata, S., 2019. Impact of field biomass burning on local pollution and long-range transport of $PM_{2.5}$ in Northeast Asia. Environ. Pollut. 244, 414–422. https://doi.org/10.1016/j.envpol.2018.09.061.
Vagg, A., 2015. Rice straw utilisation-Value adding and alternative uses for the Australian rice industry. A Report for Nuffield Australia Farming Scholars Nuffield Australia.
Wang, Y.L., Wild, O., Chen, H.S., Gao, M., Wu, Q.Z., Qi, Y., Chen, X.S., Wang, Z.F., 2020. Acute and chronic health impacts of $PM_{2.5}$ in China and the influence of interannual meteorological variability. Atmos. Environ. 229, 117397. https://doi.org/10.1016/j.atmosenv.2020.117397.
Wiedinmyer, C., Quayle, B., Geron, C., Belote, A., McKenzie, D., Zhang, X., O'Neill, S., Wynne, K.K., 2006. Estimating emissions from fires in North America for air quality modeling. Atmos. Environ. 40 (19), 3419–3432. https://doi.org/10.1016/j.atmosenv.2006.02.010.
Wiedinmyer, C., Akagi, S.K., Yokelson, R.J., Emmons, L.K., Al-Saadi, J.A., Orlando, J.J., Soja, A.J., 2011. The Fire INventory From NCAR (FINN): A High Resolution Global Model to Estimate the Emissions From Open Burning. 8. Chemistry and Biochemistry Faculty Publications.
Woody, M.C., Baker, K.R., Hayes, P.L., Jimenez, J.L., Koo, B., Pye, H.O., 2016. Understanding sources of organic aerosol during CalNex-2010 using the CMAQ-VBS. Atmos. Chem. Phys. 16 (6), 4081–4100. https://doi.org/10.5194/acp-16-4081-2016.
Wu, J., Zhang, P., Yi, H., Qin, Z., 2016. What causes haze pollution? An empirical study of $PM_{2.5}$ concentrations in Chinese cities. Sustainability 8, 132. https://doi.org/10.3390/su8020132.
Wu, L., Wang, X., Lu, S., Shao, M., Ling, Z., 2019. Emission inventory of semi-volatile and intermediate-volatility organic compounds and their effects on secondary organic aerosol over the Pearl River Delta region. Atmos. Chem. Phys. 19 (12), 8141–8161. https://doi.org/10.5194/acp-19-8141-2019.
Xie, R., Sabel, C.E., Lu, X., Zhu, W., Kan, H., Nielsen, C.P., Wang, H., 2016. Long-term trend and spatial pattern of $PM_{2.5}$ induced premature mortality in China. Environ. Int. 97, 180–186. https://doi.org/10.1016/j.envint.2016.09.003.
Yang, G., Zhao, H., Tong, D.Q., Xiu, A., Zhang, X., Gao, C., 2020. Impacts of post-harvest open biomass burning and burning ban policy on severe haze in the

Northeastern China. Sci. Total Environ. 716, 136517. https://doi.org/10.1016/j.scitotenv.2020.136517.
Yevich, R., Logan, J.A., 2003. An assessment of biofuel use and burning of agricultural waste in the developing world. Glob. Biogeochem. Cycles 17 (4), 1095. https://doi.org/10.1029/2002GB001952.
Yin, S., Guo, M., Wang, X.F., Yamamoto, H., Ou, W., 2021. Spatiotemporal variation and distribution characteristics of crop residue burning in China from 2001 to 2018. Environ. Pollut. 268, 115849. https://doi.org/10.1016/j.envpol.2020.115849.
Zha, S., Zhang, S., Cheng, T., Chen, J., Huang, G., Li, X., Wang, Q., 2013. Agricultural fires and their potential impacts on regional air quality over China. Aerosol Air Qual. Res. 13 (3), 992–1001. https://doi.org/10.4209/aaqr.2012.10.0277.
Zhang, J.J., Cui, M.M., Fan, D., Zhang, D.S., Lian, H.X., Yin, Z.Y., Li, J., 2015. Relationship between haze and acute cardiovascular, cerebrovascular, and respiratory diseases in Beijing. Environ. Sci. Pollut. Res. 22 (5), 3920–3925. https://doi.org/10.1007/s11356-014-3644-7.
Zhao, B., Wang, S., Donahue, N.M., Jathar, S.H., Huang, X., Wu, W., Hao, J., Robinson, A.L., 2016. Quantifying the effect of organic aerosol aging and intermediate-volatility emissions on regional-scale aerosol pollution in China. Sci. Rep. 6, 28815. https://doi.org/10.1038/srep28815.
Zhou, Y., Xing, X., Lang, J., Chen, D., Cheng, S., Wei, L., Wei, X., Liu, C., 2017. A comprehensive biomass burning emission inventory with high spatial and temporal resolution in China. Atmos. Chem. Phys. 17 (4), 2839–2864. https://doi.org/10.5194/acp-17-2839-2017.
Zhou, Y., Han, Z., Liu, R., Zhu, B., Li, J., Zhang, R., 2018. A modeling study of the impact of crop residue burning on $PM_{2.5}$ concentration in Beijing and Tianjin during a severe autumn haze event. Aerosol Air Qual. Res. 18 (7), 1558–1572. https://doi.org/10.4209/aaqr.2017.09.0334.
Zong, Z., Wang, X., Tian, C., Chen, Y., Qu, L., Ji, L., Zhi, G., Li, J., Zhang, G., 2016. Source apportionment of $PM_{2.5}$ at a regional background site in North China using PMF linked with radiocarbon analysis: insight into the contribution of biomass burning. Atmos. Chem. Phys. 16 (17), 11249–11265. https://doi.org/10.5194/acp-16-11249-2016.